

SANDIA REPORT

SAND87-2067 • UC-80

Unlimited Release

Printed October 1987

RS-8232-2/66432

cy 1

Specific Power of Liquid-Metal-Cooled Reactors



8232-2/066432



00000001 -

Dean Dobranich

Prepared by
Sandia National Laboratories
Albuquerque, New Mexico 87185 and Livermore, California 94550
for the United States Department of Energy
under Contract DE-AC04-76DP00789



Issued by Sandia National Laboratories, operated for the United States Department of Energy by Sandia Corporation.

NOTICE: This report was prepared as an account of work sponsored by an agency of the United States Government. Neither the United States Government nor any agency thereof, nor any of their employees, nor any of their contractors, subcontractors, or their employees, makes any warranty, express or implied, or assumes any legal liability or responsibility for the accuracy, completeness, or usefulness of any information, apparatus, product, or process disclosed, or represents that its use would not infringe privately owned rights. Reference herein to any specific commercial product, process, or service by trade name, trademark, manufacturer, or otherwise, does not necessarily constitute or imply its endorsement, recommendation, or favoring by the United States Government, any agency thereof or any of their contractors or subcontractors. The views and opinions expressed herein do not necessarily state or reflect those of the United States Government, any agency thereof or any of their contractors or subcontractors.

Printed in the United States of America
Available from
National Technical Information Service
U.S. Department of Commerce
5285 Port Royal Road
Springfield, VA 22161

NTIS price codes
Printed copy: A03
Microfiche copy: A01

SPECIFIC POWER OF LIQUID-METAL-COOLED REACTORS

Dean Dobranich
Advanced Nuclear Power Systems Safety Division
Sandia National Laboratories
Albuquerque, New Mexico 87185

ABSTRACT

Calculations of the core specific power for conceptual space-based liquid-metal-cooled reactors, based on heat transfer considerations, are presented for three different fuel types: (1) pin-type fuel, (2) cermet fuel, and (3) thermionic fuel. The calculations are based on simple models and are intended to provide preliminary comparative results. The specific power is of interest because it is a measure of the core mass required to produce a given amount of power. Potential problems concerning zero-g critical heat flux and loss-of-coolant accidents are also discussed because these concerns may limit the core specific power. Insufficient experimental data exists to accurately determine the critical heat flux of liquid-metal-cooled reactors in space; however, preliminary calculations indicate that it may be a concern. Results also indicate that the specific power of the pin-type fuels can be increased significantly if the gap between the fuel and the clad is eliminated. Cermet reactors offer the highest specific power because of the excellent thermal conductivity of the core matrix material. However, it may not be possible to take full advantage of this characteristic when loss-of-coolant accidents are considered in the final core design. The specific power of the thermionic fuels is dependent mainly on the emitter temperature. The small diameter thermionic fuels have specific powers comparable to those of pin-type fuels.

ACKNOWLEDGMENTS

The author would like to thank Albert Marshall, Vincent Dandini, and Steve Webb for their comments concerning this work.

CONTENTS

	page
ABSTRACT	i
ACKNOWLEDGMENTS	ii
1.0 INTRODUCTION	1
2.0 SPECIFIC POWER FORMULAE	2
2.1 Pin-Type Fuel	3
2.2 Cermet Fuel	5
2.3 Thermionic Fuel	8
3.0 HEAT TRANSFER COEFFICIENTS	10
4.0 SPECIFIC POWER CALCULATIONS	12
5.0 CRITICAL HEAT FLUX CONCERNS	19
6.0 LOSS-OF-COOLANT CONCERNS	22
7.0 SUMMARY	27
8.0 REFERENCES	28

1.0 INTRODUCTION

Liquid-metal-cooled nuclear reactors have been proposed for use in outer space to supply tens of megawatts of thermal power for the production of electricity to power various defense-related space platforms. An item of concern for any space-based component is its weight because of the associated high launch costs. Thus, the determination of the weight required by a reactor core to produce a given amount of power is a parameter of interest. A measure of this parameter is the specific power defined as the maximum amount of power a unit mass of fuel can produce for a particular set of operating conditions. The RSMASS code [1] is used to provide estimates of the reactor and shield masses for space-based nuclear reactors. One of the required input variables for RSMASS is the specific power (MW/kg-U) of the reactor. Recently completed thermal hydraulic analyses [2,3] provided estimates of specific power for several gas-cooled reactors. A similar analysis has been carried out for liquid-metal-cooled reactors and the results of this analysis are reported in this report. The analysis was performed for three types of fuels: (1) pin-type fuel, (2) cermet fuel, and (3) thermionic fuel. The effect of critical heat flux constraints is also addressed along with a simple analysis of a loss-of-coolant accident and its possible impact on the specific power.

2.0 SPECIFIC POWER FORMULAE

With respect to heat transfer, the specific power for the liquid-metal-cooled reactors is a function of the thermal resistances associated with core components such as the fuel, the gap, the fuel cladding or coating, and the coolant. With the coolant and the maximum-allowed fuel temperatures specified, the specific power, P_s , can be expressed as:

$$P_s = (T_f - T_c) / (\rho_f P_z P_r \sum_{i=1}^n R_i) \quad (1)$$

where: T_f = maximum-allowed fuel temperature,
 T_c = coolant bulk temperature (or fuel surface temperature) at fuel hot spot,
 ρ_f = fuel density,
 P_z = axial peak-to-average power factor,
 P_r = radial peak-to-average power factor,
 n = the number of core thermal resistances, and
 R_i = the i^{th} thermal resistance.

The thermal resistances were derived for this work on a unit volume basis as opposed to a unit area basis as is commonly found in the heat transfer literature. This was done because the quantity of interest (the specific power) is determined as the fuel volumetric heat generation rate divided by the fuel density. Therefore, expressing the resistances on a volume basis is consistent with the objective of this work and makes the evaluation of equation (1) straightforward.

If a cosine axial power profile is assumed, the coolant bulk temperature at the fuel hot spot can be estimated as the algebraic average of the core inlet and outlet coolant temperatures. For a flat axial profile, the core outlet coolant temperature should be used. If a boiling coolant is used, then the saturation temperature provides a good estimate of the coolant bulk temperature.

Several multimegawatt space reactor concepts have been proposed that use a liquid metal to provide core cooling. In some concepts, the metal remains a liquid as it passes through the core while other concepts make use of boiling liquid-metal coolant. Three basic fuel types have been proposed for the liquid-metal-cooled reactors: (1) pin-type fuel in which the fuel is in the form of clad fuel pins, (2) cermet fuel in which a ceramic fuel resides in a metal matrix material such as tungsten, and (3) thermionic fuel in which the fuel is in the form of clad hollow cylindrical pins. In the pin-type fuel, coolant flows within the space between the fuel rods. In the cermet fuel, the coolant flows either axially or radially through channels formed within the matrix material. In the thermionic fuel, coolant flows around a collector that surrounds

the hollow pin. (The hole in the fuel pin provides volume for the collection of fission products and the outer surface of the cladding is the thermionic emitter.)

The formulae used to determine specific power for the three types of fuels are presented in the next three subsections.

2.1 Pin-Type Fuel

A schematic diagram of the pin-type fuel is given in Figure 2.1.1. A liner material is shown between the fuel and the gap. The thermal resistance for the liner should be neglected if a liner is not used for a particular concept. The thermal resistances, R , associated with the pin-type geometry are as follows:

fuel
pin:

$$R_f = r_1^2 / 4k_f \quad (2)$$

liner:

$$R_l = r_1^2 \ln(r_2/r_1) / 2k_l \quad (3)$$

gap:

$$R_g = r_1^2 / 2r_2 h_g \quad (4)$$

clad:

$$R_{cl} = r_1^2 \ln(r_4/r_3) / 2k_{cl} \quad (5)$$

coolant:

$$R_c = r_1^2 / 2r_4 h_c \quad (6)$$

where; r = radius,
 h = heat transfer coefficient, and
 k = thermal conductivity.

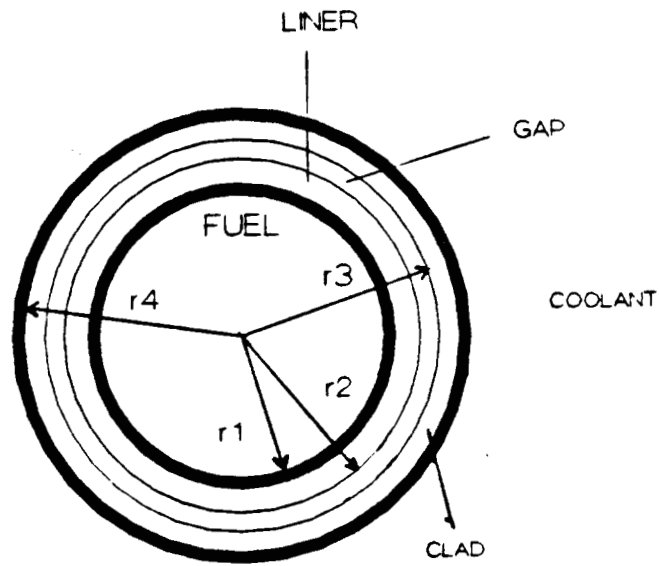


Figure 2.1.1 Pin-Type Fuel Schematic

2.2 Cermet Fuel

A schematic diagram of the cermet fuel type is given in Figure 2.2.1. The expressions for the thermal resistances associated with this fuel type are not straightforward because the fuel is dispersed within the matrix material either as a composite or as coated spherical particles. If the fuel is dispersed as a composite, the resistances associated with the particle and coating do not apply. The distance S , as shown in Figure 2.2.1, is the maximum distance that heat must travel from the fuel to the coolant channel wall. A fuel particle is assumed to reside at this location to provide a conservative estimate (worst case) of the matrix and particle temperature differences. Because the fuel is uniformly dispersed within the matrix material, the matrix is assumed to have a uniform volumetric heat generation rate. An estimate of the matrix temperature drop across the distance S can be made by using the conduction relation for heat flow in a hollow cylinder of inside radius equal to the channel radius and outside radius equal to the inside radius plus the distance S . Assuming circular channels of constant flow area, the resistances are as follows:

fuel

particle:

$$R_{\text{par}} = d_{\text{par}}^2 / 24k_f \quad (7)$$

coating:

$$R_{\text{ct}} = t d_{\text{par}}^2 / [12k_{\text{ct}}(d_{\text{par}}/2 + t)] \quad (8)$$

matrix:

$$R_m = [G(S + d_c)^2 - B/2] fV_f / 2k_m \quad (9)$$

coolant:

$$R_c = BfV_f / h_c d_{\text{ch}} \quad (10)$$

$$\text{with; } G = \ln[(2S + d_{\text{ch}}) / d_{\text{ch}}] \quad (11)$$

$$B = [(S + d_{\text{ch}}/2)^2 - (d_{\text{ch}}/2)^2] \quad (12)$$

where; V_f = fuel volume fraction

f = geometry correction factor

S = maximum matrix conduction length,

t = coating thickness, and

d = diameter.

As previously mentioned, the maximum matrix conduction length, S , is the maximum distance that heat must travel from the fuel to the coolant channel wall and depends on the number and diameter of the channels, and whether the channels are arranged on a triangular or square array. Figure 2.2.1 provides examples of these two arrangements. The area bounded by the circle of diameter $d_{\text{ch}} + 2S$ represents the unit cell for the

heat conduction calculations. The geometric unit cell is shown as a hexagon for the triangular array and as a square for the square array.

The geometry correction factor, f , accounts for the fact that the conduction unit cell volume is larger than the geometric unit cell volume. The geometric correction factor can be calculated as the cross-sectional area of the geometric unit cell (not including the channel area) divided by the cross-sectional area of the conduction unit cell (again, not including the channel area). In dealing with reactor concepts, f will in general not be known because it depends on the number and spacing of the channels. However, f will be less than 1.0, and using f equal to 1.0 results in a conservative estimate of specific power; i.e., the actual specific power will be somewhat larger.

The fuel volume fraction, V_f , is defined as the volume of fuel divided by the volume of matrix material. This is a measure of the fuel loading within the core and must be based not only on specific power constraints but also on criticality constraints. Lower values of V_f result in higher values of specific power.

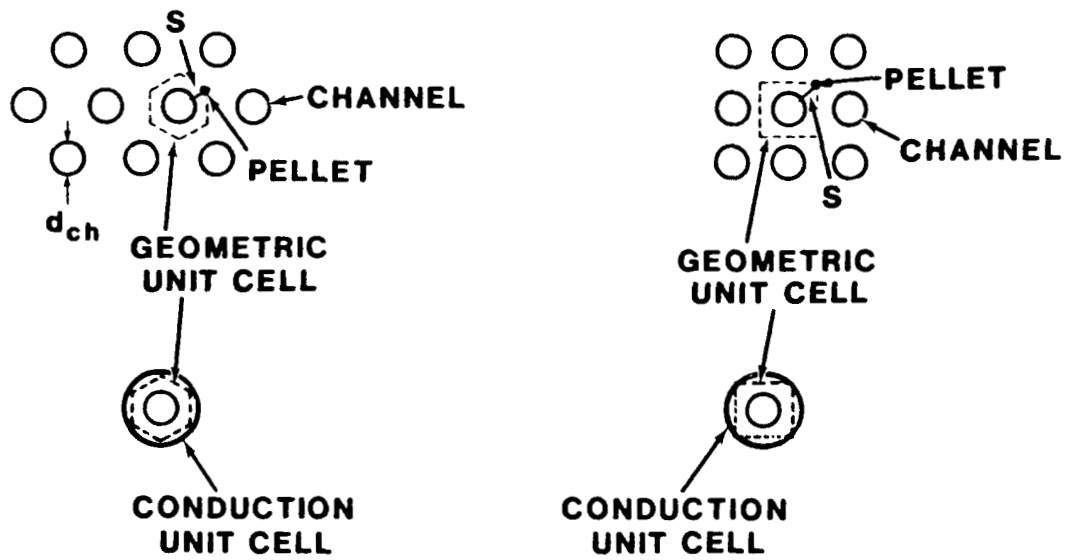


Figure 2.2.1 Matrix Fuel Schematic
(Triangular and Square Arrays)

2.3 Thermionic Fuel

A schematic of the thermionic fuel is shown in Figure 2.3.1. Thermionic fuel produces electric power by "boiling" electrons off the surface of an emitter material; the electrons are then collected on a collector surface. There is a gap between the emitter and collector surfaces, and the collector is surrounded by the coolant. For the thermionic fuel, the outer clad surface as shown in the figure is the emitter. The emitter temperature defines the operating characteristics of the thermionic fuel and is assumed to be specified for the specific power calculations. Therefore, the collector and coolant temperatures do not enter into the specific power calculations; only the maximum-allowed fuel temperature (at radius r_1) and the emitter temperature (at radius r_3) are needed. The thermal resistances for the thermionic fuel are:

fuel
pin:

$$R_f = [(r_2^2 - r_1^2)/2 - r_1^2 \ln(r_2/r_1)] / (2k_f) \quad (13)$$

clad:

$$R_{cl} = (r_2^2 - r_1^2) \ln(r_3/r_2) / (2k_{cl}) \quad (14)$$

where; r = radius, and
 k = thermal conductivity.

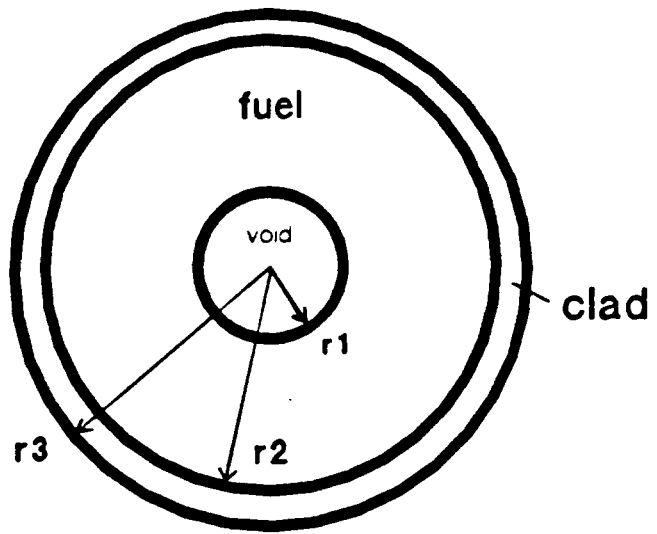


Figure 2.3.1 Thermionic Fuel Schematic

3.0 HEAT TRANSFER COEFFICIENTS

To calculate the thermal resistances, values for the various parameters appearing in the resistance formulae must be provided. The parameters consist of (1) dimensions, which are related to the core geometry, (2) thermal conductivities, which are related to the materials used in the core, and (3) the heat transfer coefficients for the gap and the coolant. The gap and coolant heat transfer coefficients are addressed in this section.

For liquid-metal-cooled reactors with pin-type fuel, the thermal resistance associated with the gap is larger than the other thermal resistances and therefore dominates the specific power limit. The gap heat transfer coefficient (or gap conductance) increases with burnup and is lowest at the beginning of core life. For light water reactors, the gap conductance, h_g , varies between about 5,000 and 30,000 $W/m^2/K$ over the life of the fuel. For liquid-metal-cooled fast reactors, h_g varies between approximately 3,000 and 20,000 $W/mq.m/K$ [4]. Because the thermal resistance associated with the gap is relatively large and because h_g varies over a wide range, h_g is best treated parametrically for conceptual reactors.

For forced convection to single-phase liquid metals, there is a wealth of heat transfer coefficient data available in the literature. Typically, the heat transfer coefficient ranges from 20,000 to 60,000 $W/m^2/K$ [5]. A popular correlation [5] for liquid-metal single-phase forced convection heat transfer is:

$$Nu = 7.0 + 0.025Pe^{0.8} \quad (15)$$

where; Nu = Nusselt number, and
 Pe = Peclet number.

Numerous correlations for liquid-metal pool boiling are also available [6]. However, there are very few correlations available for forced convection boiling, and the uncertainties associated with the available correlations are large. A correlation for forced convection liquid-metal boiling [7] is given by:

$$h = 0.204[L(x_n - 2x_1)]^{0.7} p^{0.15} (Gd/l)^{0.7} \quad (16)$$

where; h = heat transfer coefficient [$W/m^2/k$],
 L = latent heat of evaporation [J/kg],
 x_n = exit quality,
 x_1 = subcooled inlet vapor quality,
 p = pressure [N/m^2],
 G = mass flow per unit flow cross section [$kg/m^2/s$],
 d = channel diameter [m], and
 l = channel length [m].

This correlation was developed for use in a one-g (earth gravity) environment; boiling heat transfer data for a zero-g environment representative of earth orbit is essentially nonexistent. Liquid metals typically possess very good heat transfer properties; therefore, for pin-type fuel with a gap, the thermal resistance associated with the coolant is small compared to the total core resistance and use of the one-g heat transfer coefficient correlation will not have a significant effect on the specific power calculations. However, for cermet fuel and for pin-type fuel without a gap, the thermal resistance associated with the coolant is a large fraction of the total. For these cases, use of the one-g data is the best that can be done until zero-g data becomes available.

4.0 SPECIFIC POWER CALCULATIONS

Some example specific power calculations are included in this section to demonstrate the use of the formulae presented in the previous sections.

Heat Transfer Coefficient for Boiling Potassium Coolant

Assumed conditions -

pressure = 1.58 MPa

$l/d = 260$

$L = 1.663E6$ J/kg

$x_1 = 0.0$

$x_n = 0.20$

$G = 1350$ kg/s/m²

Calculated heat transfer coefficient:

$h_C = 40,000$ W/m²/K

Specific Power for Pin-Type Fuel

Fuel Density - 13600 kg/m³

$P_z = P_r = 1.0$

Dimensions:

$r_1 = 0.002213$ m

$r_2 = 0.002340$ m

$r_3 = 0.002540$ m

$r_4 = 0.003175$ m

Conductivities:

fuel (Uranium Nitride): $k_f = 26.0$ W/m/K

liner (Tungsten): $k_l = 110$ W/m/K

clad (Niobium alloy): $k_{cl} = 54$ W/m/K

Heat transfer coefficients:

gap - 5000 W/m²/K

coolant - 40,000 W/m²/K

Temperatures:

Fuel centerline - 1600 K

Coolant bulk - 1450 K

Calculated resistances (K-m³/W):

$R_f = 4.71E-8$
 $R_l = 1.24E-9$
 $R_g = 2.09E-7$
 $R_{Cl} = 1.01E-8$
 $R_C = 1.93E-8$
Total = 2.87E-7

Calculated specific power:

$P_s = 0.038 \text{ MW/kg}$

If the maximum-allowed fuel centerline temperature is increased to 2000 K, the specific power increases to 0.141 MW/kg. If in addition to increasing the fuel temperature the gap is eliminated, the specific power increases to 0.519 MW/kg. (Elimination of the gap may be possible for reactors designed for short operation times.)

Specific Power for Cermet Fuel

Fuel Density - 13600 kg/m³
 $V_f = 0.35$
 $P_z = P_r = 1.0$

Dimensions:

$d_{ch} = 0.004 \text{ m}$
 $S = 0.0013 \text{ m}$
 $d_{par} = 0.0001 \text{ m}$
 $t^r = 0.0$

Conductivities:

fuel (Uranium Nitride): $k_f = 26.0 \text{ W/m/K}$
matrix (Tungsten): $k_m = 110 \text{ W/m/K}$

Heat transfer coefficient:

coolant - 40,000 W/m²/K

Temperatures:

Fuel centerline - 1750 K
Coolant bulk - 1350 K

Calculated resistances (K-m³/W):

$R_{par} = 1.6E-11$
 $R_m = 3.20E-9$
 $R_C = 1.51E-8$
Total = 1.83E-8

Calculated specific power:

$$P_s = 1.606 \text{ MW/kg}$$

This calculation shows that with a cermet fuel, the resistances associated with the core are less than in the case of pin-type fuels containing a gap. Thus, for the cermet fuel, heat transfer to the coolant accounts for a large fraction of the total thermal resistance.

The example calculations are for a boiling liquid metal; however, these specific power values would be about the same for either a boiling or non-boiling liquid-metal coolant because the coolant heat transfer coefficients would be comparable.

Specific Power for Thermionic Fuel

Fuel Density - 10500 kg/m^3

$$P_z = P_r = 1.0$$

Dimensions:

$$r_1 = 0.00192 \text{ m}$$

$$r_2 = 0.00525 \text{ m}$$

$$r_3 = 0.00585 \text{ m}$$

Conductivity:

fuel (Uranium Dioxide): $k_f = 2.6 \text{ W/m/K}$

clad (Tungsten): $k_{cl} = 110 \text{ W/m/K}$

Temperatures:

Fuel inner surface - 2900 K

Clad outer surface - 1960 K

Calculated Resistance ($\text{K-m}^3/\text{W}$)

$$R_f = 1.58\text{E-}6$$

$$R_{cl} = 1.17\text{E-}8$$

$$\text{Total} = 1.59\text{e-}6$$

Calculated Specific Power:

$$P_s = 0.056 \text{ MW/kg}$$

If the clad outer surface temperature (emitter) is increased to 2400 K , the specific power decreases to 0.030 MW/kg .

In addition to the previous example calculations, parametric calculations were performed to determine the effect on specific power of coolant temperature and maximum-allowed fuel temperature for pin-, cermet-, and thermionic-type fuels. Also, for pin-type fuel, the effect of gap conductance was determined and for cermet fuel, the effect of the coolant heat transfer coefficient was calculated. For the thermionic fuel, the effect of fuel dimensions and emitter temperature were investigated. The results of these calculations are presented in Figures 4.1 through 4.6. These results apply for both the boiling and non-boiling cases because the coolant heat transfer coefficients are of the same order of magnitude for the two cases. Given the conceptual nature of the reactor designs and the uncertainty associated with liquid-metal boiling in a zero-g environment, the use of significantly different heat transfer coefficients is not warranted.

Figure 4.1 shows the specific power as a function of coolant temperature for pin-type fuel. The curves were generated both with and without a gap for two different maximum fuel temperatures. (A gap conductance of $5 \text{ kW/m}^2/\text{K}$ was used for the with-gap cases.) The two curves for the no-gap cases show higher specific powers than the two curves for the with-gap cases because the relatively large thermal resistance associated with the gap has been eliminated. Figure 4.2 demonstrates the dependence of specific power on the gap conductance for the pin-type fuel.

Figures 4.3 and 4.4 show the specific power for the cermet fuel reactors with coolant heat transfer coefficients of 40 and $60 \text{ kW/m}^2/\text{K}$, respectively. The specific power curves are presented as a function of coolant temperature and maximum fuel temperature. The cermet reactors do not have a gap; therefore, the thermal resistance associated with the coolant is a larger fraction of the total thermal resistance compared to the pin-type fuel. Increases in the coolant heat transfer coefficient are therefore more beneficial for the cermet reactors.

Figure 4.5 shows the specific power as a function of maximum-allowed fuel temperature and emitter temperature for the thermionic fuel. Increasing the emitter temperature is desirable with respect to increasing the efficiency of the thermionic process; however, higher emitter temperatures result in a decrease in the specific power. Figure 4.6 shows the specific power as a function of emitter temperature for three different fuel outer radius values. (For these calculations, the void space radius, r_1 , was adjusted such that r_1^2/r_2^2 was constant.) This figure shows that smaller fuel pins have a greater potential for achieving higher specific power.

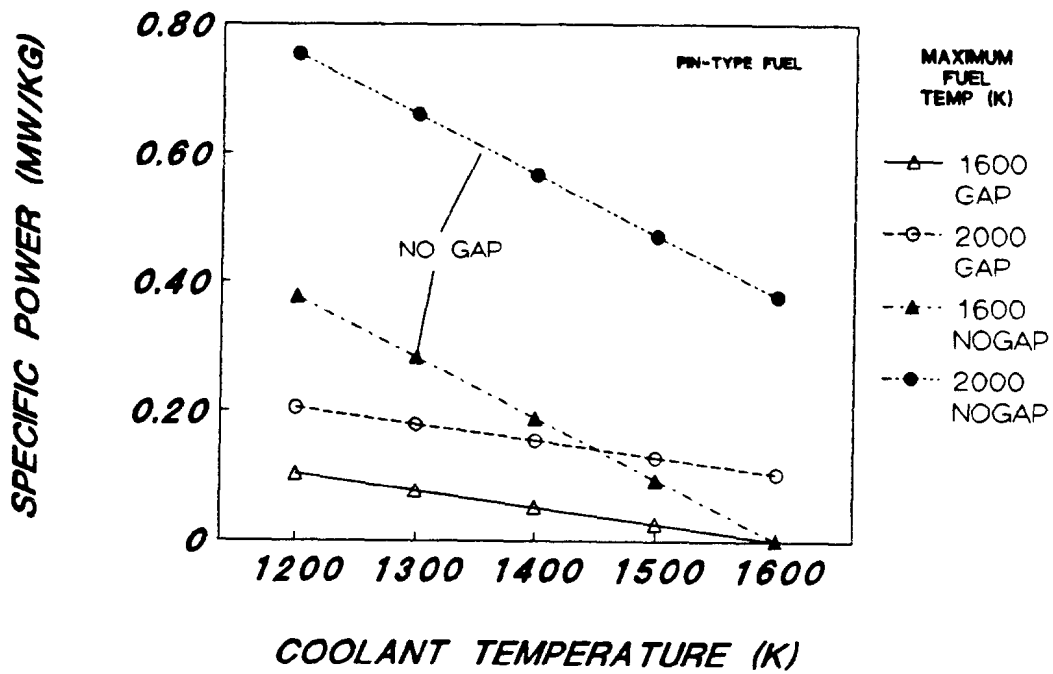


Figure 4.1 Specific Power for Pin-Type Fuel (Gap Conductance of 5 kW/m²/K)

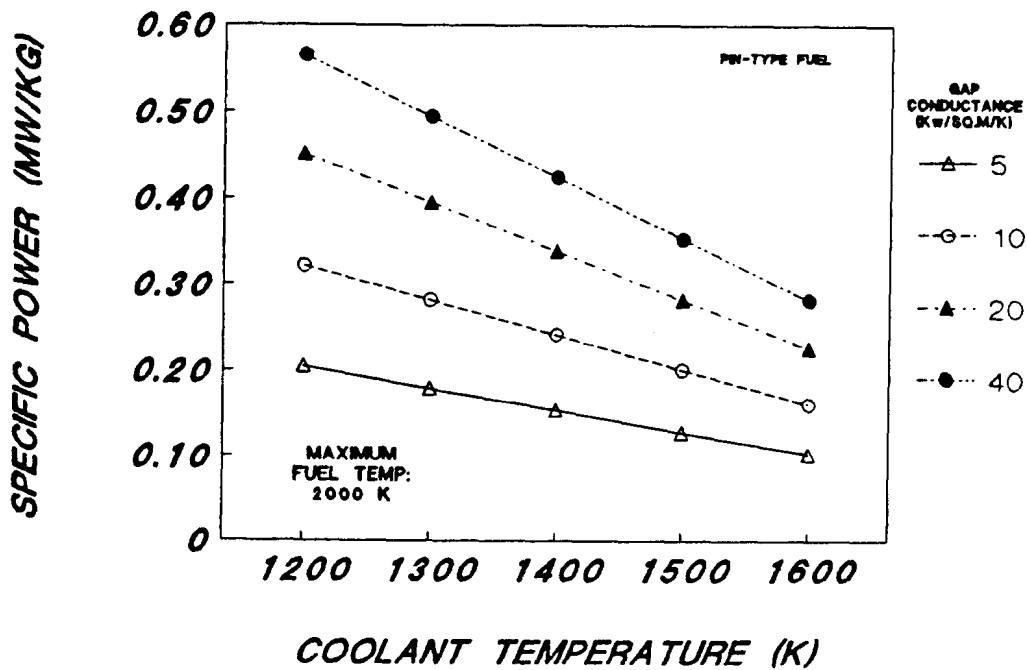


Figure 4.2 The Effect of Gap Conductance on Specific Power for Pin-Type Fuel (Maximum Fuel Temperature of 2000 K)

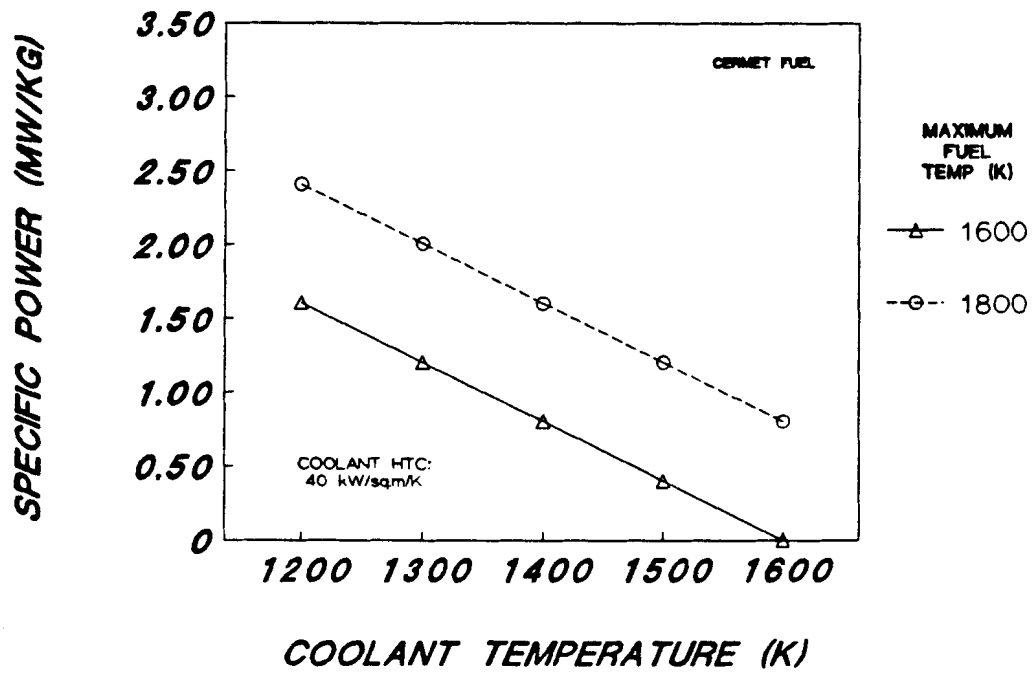


Figure 4.3 Specific Power for Cermet Fuel
(Coolant Heat Transfer Coefficient = 40 kW/m²/K)

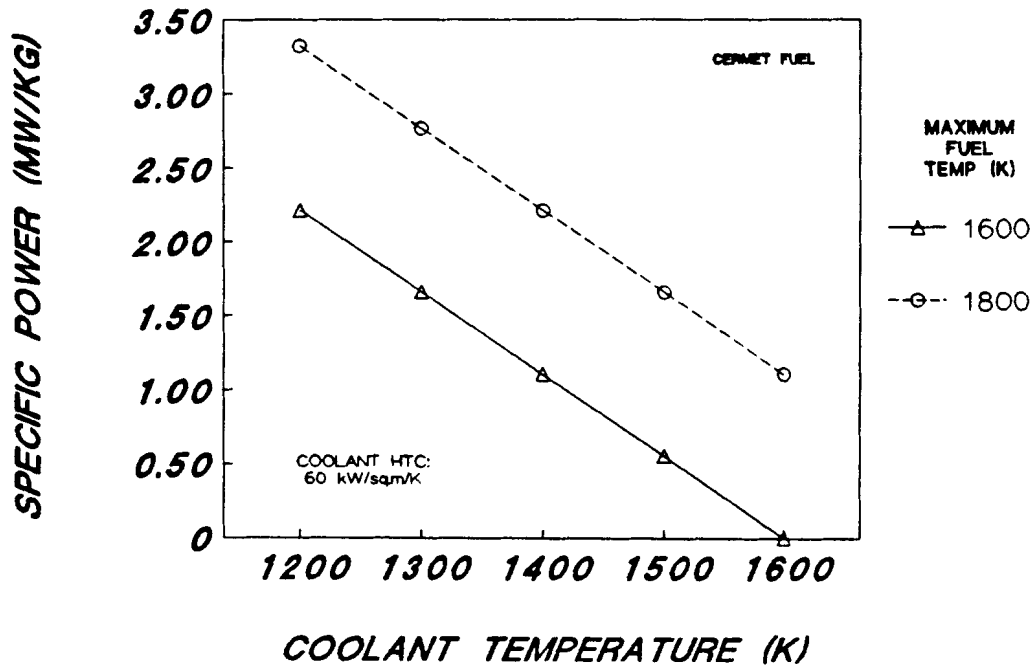


Figure 4.4 Specific Power for Cermet Fuel
(Coolant Heat Transfer Coefficient = 60 kW/m²/K)

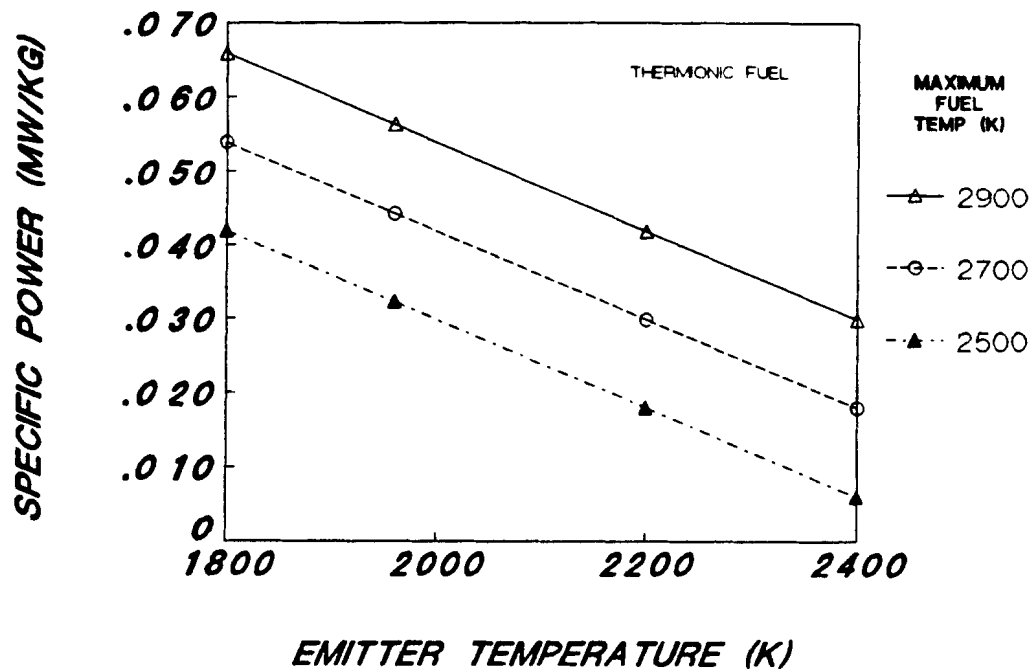


Figure 4.5 Specific Power for Thermionic Fuel

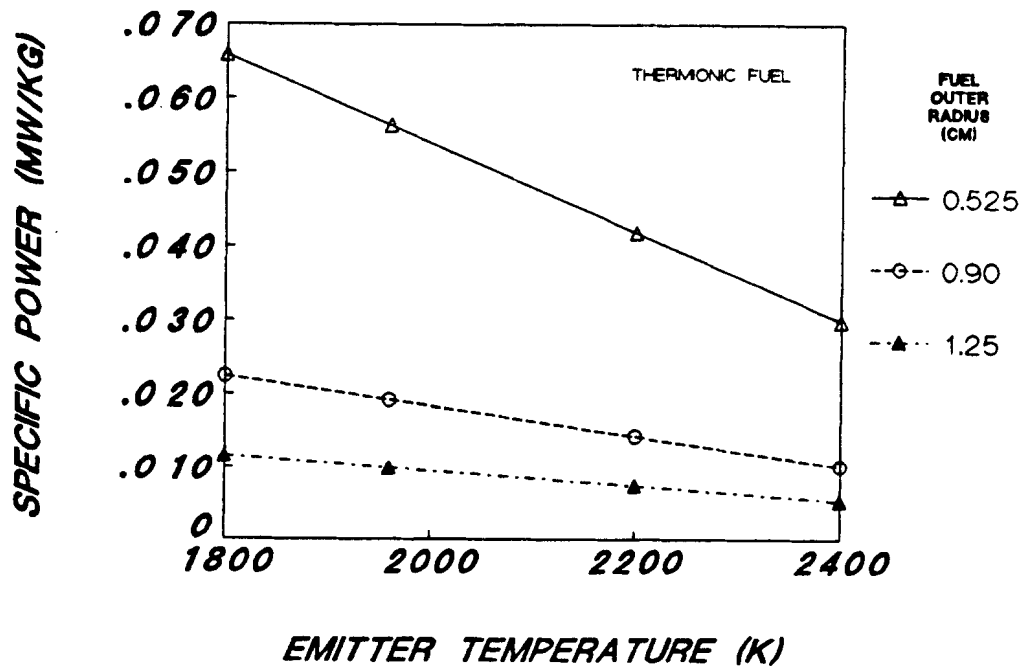


Figure 4.6 The Effect of Fuel Dimensions on the Specific Power of Thermionic Fuel (Maximum Fuel Temperature of 2900 K)

5.0 CRITICAL HEAT FLUX CONCERNS

A problem that arises with boiling liquid-metal-cooled reactors is the determination of the critical heat flux, especially in a zero-g environment. The maximum heat flux occurring at any location in the core can not exceed the critical heat flux if dryout is to be avoided. Dryout would lead to possible fuel or cladding damage. Boiling water reactors typically operate such that the maximum heat flux is a factor of about two below the critical heat flux to provide a margin of safety during normal operation. For space-based liquid-metal-cooled reactors, it is possible that the requirement to maintain the maximum heat flux below the critical heat flux will limit the specific power.

A correlation for critical heat flux [7] in a one-g environment with liquid metals at pressures below 2 bars is given by:

$$q_c'' = 0.216L(1 - 2x_1)G^{0.807}(d/l)^{0.807} \quad (17)$$

where; q_c'' = critical heat flux [W/m^2].

Critical heat flux correlations for liquid metals in a zero-g environment do not exist. Even the available data for two-phase heat transfer in zero-g for common fluids such as water is very limited. However, the available evidence seems to indicate that the critical heat flux will be lower in a reduced gravity environment than in a one-g environment. Figure 5.1 [8] shows the critical heat flux at reduced gravity divided by the critical heat flux at earth gravity for several fluids. Figure 5.2 [8] shows the boiling curve for several fluids at one-g and at reduced g. These figures indicate that the zero-g critical heat flux is reduced by roughly a factor of three. It must be noted that both Figures 5.1 and 5.2 are based on pool boiling experiments. The effects on forced-flow critical heat flux at reduced gravity are really not known. However, there is some evidence to indicate that for high flow rates, the reduction in critical heat flux associated with reduced gravity will be less for forced convection boiling than for pool boiling. It is not clear how great the flow rate must be to suppress the possible detrimental effects associated with reduced gravity.

The peak heat flux for a reactor core can be expressed as:

$$q_p'' = P_z P_r 0.25(Gd/l)[c_p(T_{sat} - T_i) + x_n L] \quad (18)$$

where; q_p'' = peak heat flux,
 c_p = specific heat,
 T_{sat} = saturation temperature, and
 T_i = core inlet temperature.

The first term in the brackets accounts for sensible heat addition and the second term accounts for latent heat addition.

The peak heat flux expression can be combined with the expression for critical heat flux to yield:

$$q_c''/q_p'' = 0.864L(1 - 2x_1)Y/[P_zP_r(c_p\Delta T + x_nL)] \quad (19)$$

$$\text{with; } Y = (l/d/G)^{0.193} \quad (20)$$

$$\text{and } \Delta T = T_{\text{sat}} - T_i \quad (21)$$

If this ratio is below some acceptable design limit, the specific power would have to be reduced accordingly. An example critical heat flux calculation is presented below for potassium coolant in a one-g environment.

Calculation of Critical Heat Flux Ratio

Assumed conditions -

pressure = 1.58 MPa
l/d = 260
 $\Delta T = 110$ K
 $c_p = 1000$ J/kg/K (Potassium)
 $L_p = 1.663E6$ J/kg
 $x_1 = 0.0$
 $x_n = 0.20$
 $G = 1350$ kg/s/m²
 $P_zP_r = 1.5$

Calculated critical heat flux ratio -

$$q_c''/q_p'' = 1.57$$

The uncertainty associated with this result is substantial given the very limited amount of test data that is available for critical heat flux along with the fact that the reactor parameters are based on a conceptual design. Also, recall that the correlation for critical heat flux was based on results for pressures below 2 bars. This result however, gives an indication that the critical heat flux constraint associated with a boiling liquid metal may be a problem, especially if the effects of zero-g prove to be detrimental.

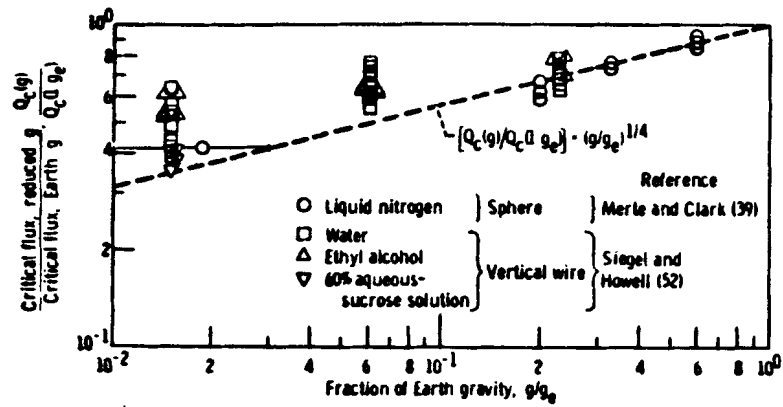


Figure 5.1 Effects of Reduced Gravity on Critical Heat Flux [8]

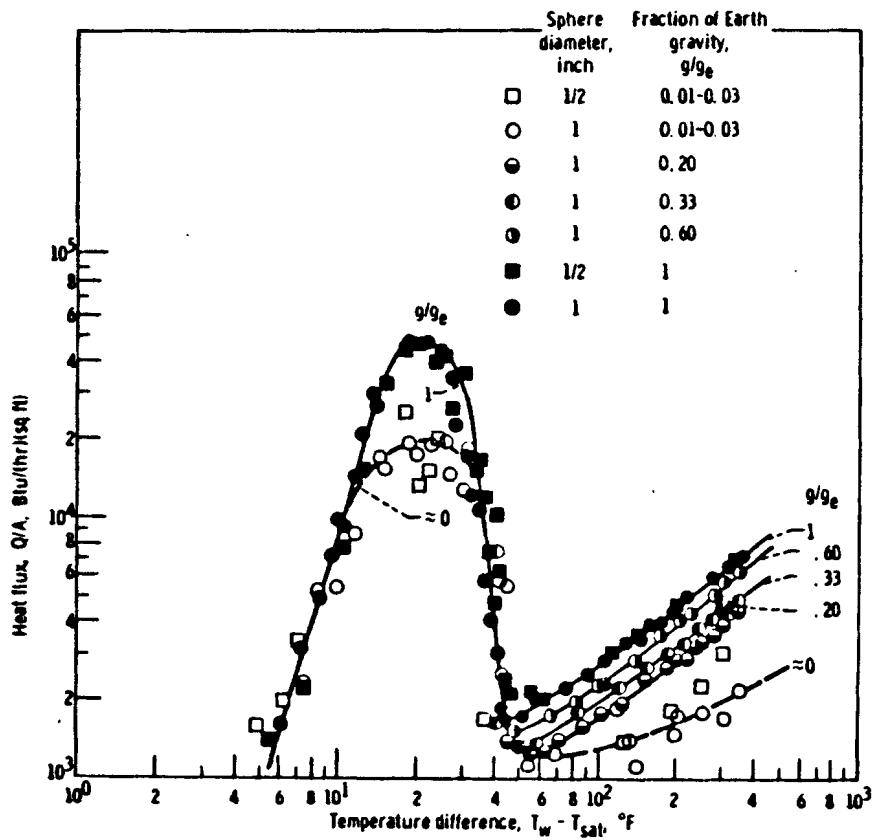


Figure 5.2 Boiling Curve at Reduced Gravity [8]

6.0 LOSS-OF-COOLANT CONCERNS

As discussed in the previous section, it might be necessary to restrict the specific power because of critical heat flux concerns. Another concern is that of core temperature response during an accident situation such as a loss-of-coolant accident. In space, one does not have the luxury of being able to collect core coolant in a sump for subsequent recirculation through the core. Once the coolant is lost, there is no easy way of providing core cooling. The only cooling mechanism readily available is by way of radiant heat transfer from the vessel to space. Prevention of fission product release dictates that the vessel remain intact; prevention of fuel melting may not be necessary but certainly would also be desirable. Thus, such safety-related concerns must be considered when determining the core specific power.

Although reactors with high specific powers enjoy the benefit of reduced weight and volume, these benefits become detriments with respect to the core's temperature response following a loss-of-coolant accident. Reduced weight results in a reduction in core heat capacity while reduced volume results in a reduction in available surface area for radiation to space. It may be necessary to reduce a core's specific power to avoid these detrimental effects.

To address this concern, a very simple loss-of-coolant accident analysis was performed for the pin-type and cermet reactors described in Section 2. A detailed analysis would require a very detailed description of the reactors and is far beyond the scope of this work. The intent of this simple analysis is to demonstrate the relative temperature response of the two types of liquid-metal-cooled reactors and thus point out possible safety-related concerns and how those concerns may effect the specific power. (Some preliminary loss-of-coolant accident analyses for low-power space reactors are presented in [10]. The work described in that reference attempts to model the effects during postulated accidents of some of the specific design details of several proposed space reactors.)

To make this otherwise difficult problem tractable, numerous assumptions and simplifications were necessary. First, it was assumed that the core is not surrounded by a vessel or any other structure and that the outer radial surface of the cylindrically shaped core radiates directly to space. Inclusion of the vessel or any other structure between the core and space (such as a neutron reflector or multifoil insulation) would introduce additional thermal resistance making heat rejection to space much more difficult and resulting in higher core temperatures. (Reference 10 provides an indication of the magnitude of these effects.)

The effective temperature of space was selected as 250 K and the emissivity of the outer core surface was chosen as 0.3. All coolant was assumed to be lost instantaneously at the start of the accident. Reactor SCRAM was also assumed to occur at the start of the accident. The ANS standard decay power function with infinite irradiation time was used to calculate the core decay power after SCRAM. Although this function was not intended for fast spectrum liquid-metal-cooled reactors, it provides a reasonable estimate of decay power for this analysis. A further assumption that was necessary for the pin-type fuel was the selection of a suitable view factor to space. Because the pins near the core center do not have a clear view of space, their view factor is essentially zero. Pins at the core periphery have a view factor of approximately 0.5 (half of their surfaces directly view space). An "effective" view factor representative of all the fuel pins was arbitrarily selected as 0.15. Again, a more detailed model would be required to accurately model this complex situation and is beyond the intent of this analysis.

The transient temperature response of the core was calculated using a lumped-parameter approach [9]. In this approach, the thermal capacitance of all of the core materials are "lumped" together to provide a single effective computational node. The differential equation describing the transient temperature response of this single node is:

$$(\rho c_p V) dT/dt = P - \sigma A(T^4 - T_s^4)/(1/\epsilon + 1/F - 1) \quad (22)$$

where; ρ = node volume-averaged density,
 c_p = node mass-averaged specific heat,
 V = node volume,
 T = node temperature,
 t = time,
 P = time-dependant core decay power,
 σ = Stefan-Boltzmann constant,
 ϵ = radiating-surface emissivity,
 F = view factor,
 A = radiating-surface area, and
 T_s = effective space temperature = 250 K.

This differential equation was solved using Euler's method [11]. The node properties for the pin-type and cermet cores, based on the information presented in Section 4, are provided in Table 6.1.

Table 6.1

Pin-Type and Cermet Core Node Properties

	<u>Pin-Type</u>	<u>Cermet</u>
Density (kg/m ³)	5912	12114
Specific Heat (J/kg/K):	260	168

The node volume, V , was determined based on the core specific powers. First, the specific power was converted to a core power density, P_d , using the following:

$$P_d = P_s \rho V_f (1 - V_c) \quad (23)$$

where; V_f = fuel volume fraction,
 V_c = core void fraction, and
 ρ = fuel density.

For the pin-type fuel, the fuel volume fraction is the fraction of the fuel rod volume occupied by fuel (UN). For the cermet fuel, it is the fraction of the solid core material volume (W and UN) occupied by fuel. The core void fraction is the fraction of the core volume normally occupied by coolant.

Using the calculated power density, the total volume of the core, V , was calculated as P/P_d . Assuming a cylindrical core with a height-to-diameter ratio of 1.0, the core diameter, D , was calculated as:

$$D = (4 V/\pi)^{1/3} \quad (24)$$

A summary of the pertinent core parameters is provided in Table 6.2 for the pin-type and cermet cores. A steady-state core power of 50 MW was assumed for both cores.

Table 6.2
 Core Parameters

	<u>Pin-Type</u>	<u>Cermet</u>
P_s (MW/kg):	0.038	1.606
V_f :	0.485	0.35
V_c :	0.45	0.30
P_d (MW/m ³):	137.8	5351.1
V (m ³):	0.3625	0.0093
D (m):	0.7728	0.2283

The calculated temperature responses for both cores are shown in Figure 6.1. Two curves are shown for the cermet core, the second curve shows the core temperature response if the power density is reduced by a factor of ten from its original value. The temperature for the pin-type core peaks at a value of 3040 K at about 22 minutes. At this time, the rate of decay power generation in the core is equal to the rate at which power is removed from the core by radiation to space. The core temperature then slowly decreases as the power continues to

decay. At approximately one minute, the cermet core temperature peaks at 5164 K which is over 2000 K higher than the pin-type core peak temperature.

If it is assumed that the peak core temperature must remain below 3000 K (the approximate melting temperature of UN), then clearly the specific power of the cermet core must be reduced. Reducing the specific power by a factor of ten reduces the peak temperature by 1964 K to a value of 3200 K. (This peak temperature occurs at about six minutes.) Thus, much of the benefit offered by cermet fuel, with respect to specific power, may be lost after safety-related concerns are addressed. A better assessment of the possible specific power penalty can be made only after complete designs of the reactors are available; it is expected that the transient temperature response will be strongly dependent on the details of the design. A more sophisticated analysis will be warranted when the design details are available.

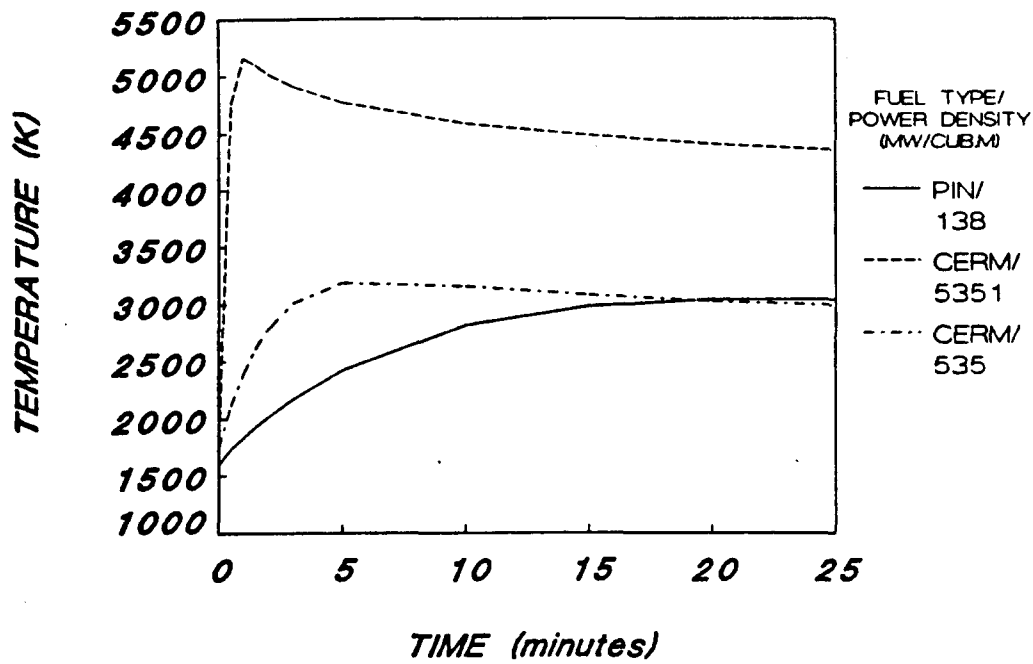


Figure 6.1 Core Temperature Response Following a Loss-of-Coolant Accident (Pin-Type and Cermet Cores)

7.0 SUMMARY

The specific power for space-based liquid-metal-cooled reactors was determined for three different fuel types: (1) pin-type fuel, (2) cermet fuel, and (3) thermionic fuel.

The specific power for the pin-type fuel ranged between about 0.04 and 0.6 MW/kg depending on the maximum-allowed fuel temperature, coolant temperature, and gap conductance. High maximum-allowed fuel temperature, low coolant temperature, and high gap conductance were most favorable with respect to specific power. Liquid metals possess good heat transfer properties, therefore, the thermal resistance associated with the coolant was relatively small. Because the thermal resistance associated with the gap dominated the total resistance, elimination of the gap resulted in significant increases in the specific power.

The specific power for the cermet fuels varied between about 1.0 and 3.5 MW/kg, again depending on the fuel and coolant temperatures. Because the cermet fuels do not have a gap and because the matrix material possesses very good thermal conductivity, the thermal resistance associated with the coolant was relatively large. Therefore, increasing the coolant heat transfer coefficient was most beneficial for the cermet fuels.

The specific power for the thermionic fuels ranged between 0.01 and 0.07 MW/kg depending on maximum-allowed fuel temperature, emitter temperature, and pin diameter. High emitter temperatures are not advantageous with respect to specific power for thermionic fuel. Large diameter pins have lower specific powers compared to the small diameter pins.

Critical heat flux data for liquid metals in a zero-g environment is essentially nonexistent. However, based on data for other fluids, it appears that critical heat flux concerns may limit the specific power for space-based liquid-metal-cooled reactors.

Another concern that may limit the specific power is the fuel temperature response following a loss-of-coolant accident. Very simplistic calculations indicated that it may be necessary to significantly reduce the core specific power in order to prevent fuel melting following such an accident. Such safety-related concerns should be considered in the design of a space-based reactor.

8.0 REFERENCES

1. Albert C. Marshall, "RSMAS: A Preliminary Reactor/Shield Mass Model for SDI Applications," SAND86-1020, August 1986.
2. Albert C. Marshall, "A Review of Gas-Cooled Reactor Concepts for SDI Applications," INF-6511-8702, Feb. 1987.
3. Dean Dobranich, "A Computer Program To Determine the Specific Power of Prismatic-Core Reactors," SAND87-0735, May 1987.
4. Y. S. Tang, R. D. Coffield, Jr., R. A. Markley, THERMAL ANALYSIS OF LIQUID METAL FAST BREEDER REACTORS, American Nuclear Society, 1978.
5. M. M. El-Wakil, NUCLEAR POWER ENGINEERING, McGraw-Hill, 1962.
6. O. E. Dwyer, BOILING LIQUID-METAL HEAT TRANSFER, American Nuclear Society, 1976.
7. H. M. Kottowski and C. Savatteri, "Fundamentals of Liquid Metal Boiling Thermohydraulics," Nuclear Engineering and Design, Vol. 82, 1984, pp. 281-304.
8. Robert Siegel, "Effects of Reduced Gravity on Heat Transfer," Advances in Heat Transfer, Vol. 4, 1967.
9. Frank Kreith, PRINCIPLES OF HEAT TRANSFER, Third Edition, Intext Educational Publishers, 1976.
10. L. N. Kmetyk, J. H. Lee, S. W. Webb, R. M. Summers and J. C. Cleveland, "Preliminary Design Considerations for Safe, On-Orbit Operations of Space Nuclear Reactors," SAND87-0865, (to be published).
11. Conte and de Boor, ELEMENTARY NUMERICAL ANALYSIS, McGraw-Hill, 1972.

DISTRIBUTION

AFAT/SAS
Fort Walton Beach, FL 32542
Attn: Capt. Jerry Brown

AFISC/SNAR
Kirtland Air Force Base
New Mexico 87117
Attn: Lt. Col. J. P. Joyce

AF Astronautics Laboratory/LKCJ
Edwards Air Force Base
MS 24
California 93523
Attn: G. Beale

AF Astronautics Laboratory/LKCJ
Edwards Air Force Base
California 93523
Attn: F. Meade

AF Astronautics Laboratory/LKCJ
Edwards Air Force Base
California 93523
Attn: Lt. R. Henley

AF Astronautics Laboratory/LKCJ
Edwards Air Force Base
California 93523
Attn: Major E. Houston

AFWAL/AA
Wright-Patterson AFB
Ohio 45433
Attn: Dick Renski

AFWAL/POOS
Wright-Patterson AFB
Bldg. 450
Ohio 45433
Attn: E. B. Kennel

AFWAL/POOC-1
Bldg. 450
Wright-Patterson AF Base
Ohio 45433
Attn: R. Thibodeau

AFWAL/POO
Aeronautical Laboratory
Wright-Patterson AFB
Ohio 45433
Attn: W. Borger

Aeronautical Laboratory
Bldg. 18
Wright-Patterson AFB
Ohio 45433
Attn: P. Colgrove

AFWAL/POOC-1
Aeronautical Laboratory
Bldg. 450
Wright-Patterson AFB
Ohio 45433
Attn: D. Massie

AFWAL/POOC-1
Aeronautical Laboratory
Wright-Patterson AFB
Ohio 45433
Attn: C. Oberly

AFWAL/POOC-1
Aeronautical Laboratory
Wright-Patterson AFB
Ohio 45433
Attn: T. Mahefky

AFWAL/POOS
Wright-Patterson AFB
Ohio 45433
Attn: J. Beam

AFWAL/POOC-1
Power Components Branch
Wright Patterson AFB
Ohio 45433-6563

AFWAL/POOC
Aeronautical Laboratory
Bldg. 18
Wright-Patterson AFB
Ohio 45433
Attn: Major Seward

AFWL/AFSC
Kirtland Air Force Base
New Mexico 87117
Attn: M. J. Schuller

AFWL/AW
Kirtland AFB
New Mexico 87117
Attn: Dr. D. Kelleher

Kirtland Air Force Base
New Mexico 87117
Attn: Lt. Col. Jackson

AFWL/AWYS
Kirtland Air Force Base
New Mexico 87117
Attn: Major D. R. Boyle

HQ AFSPACECOM/XPXIS
Peterson Air Force Base
Colorado 80914-5001
Attn: Lt. Col. F. Lawrence

HQ USAF/RD-D
Washington, DC 20330-5042
Attn: Maj. P. Talty

Aerospace Corporation
Bldg. 497, Rm. 123
P. O. Box 9113
Albuquerque, NM 87119
Attn: W. Zelinski

Aerospace Corporation
P. O. Box 9113
Albuquerque, NM 87119
Attn: W. Blocker

Aerospace Corporation
P. O. Box 9113
Albuquerque, NM 87119
Attn: M. Firmin

Aerospace Corporation
P. O. Box 92957
El Segundo, CA 90009
Attn: P. Margolis

Air Force Center for Studies
and Analyses/SASD
The Pentagon, Room ID-431
Washington, DC 20330-5420
Attn: W. Barattino, AFCSA/SASD

Air Force Foreign Technology Div.
TQTD
Wright-Patterson AFB
Ohio 45433-6563
Attn: Dr. B. L. Ballard

TQTD
Wright-Patterson AFB
Ohio 45433-6563
Attn: K. W. Hoffman

Air Force Space Technology Center
SWL
Kirtland AFB, NM 87117-6008
Attn: Capt. M. Brasher

Air Force Space Technology Center
SWL
Kirtland AFB, NM 87117-6008
Attn: J. DiTucci

Air Force Space Technology Center
SWL
Kirtland AFB, NM 87117-6008
Attn: Capt. E. Fornoles

Air Force Space Technology Center
TP
Kirtland AFB, NM 87117-6008
Attn: M. Good

Air Force Space Technology Center
XLP
Kirtland AFB, NM 87117-6008
Attn: A. Huber

Air Force Space Technology Center
SWL
Kirtland AFB, NM 87117-6008
Attn: Capt. S. Peterson

ANSER Corp.
Crystal Gateway 3
1225 Jefferson Davis Highway #800
Arlington, VA 22208
Attn: K. C. Hartkay

Argonne National Laboratory
9700 S. Cass Avenue
Argonne, IL 60439
Attn: Dr. Samit K. Bhattacharyya

Argonne National Laboratory
9700 S. Cass Avenue
Argonne, IL 60439
Attn: D. C. Fee

9700 S. Cass Avenue
Argonne, IL 60439
Attn: K. D. Kuczen

Argonne National Laboratory
9700 S. Cass Avenue
Argonne, IL 60439
Attn: Dr. R. A. Lewis

Argonne National Laboratory
9700 S. Cass Avenue
Argonne, IL 60439
Attn: D. C. Wade

Auburn University
202 Sanform Hall
Auburn, AL 36849-3501
Attn: Dr. T. Hyder

Auburn University
231 Leach Center
Auburn, AL 36849-3501
Attn: Dr. F. Rose

Avco Research Laboratory
2385 Revere Beach Pkwy
Everett, Mass. 02149
Attn: D. W. Swallow

Babcock & Wilcox
Nuclear Power Division
3315 Old Forest Road
P.O. Box 10935
Lynchburg, VA 24506-0935
Attn: B. J. Short

Battelle Pacific Northwest Lab.
P. O. Box 999
Richland, WA 99352
Attn: J. O. Barner

Battelle Pacific Northwest Lab.
P. O. Box 999
Richland, WA 99352
Attn: Dr. L. Schmid

Battelle Pacific Northwest Lab.
P. O. Box 999
Richland, WA 99352
Attn: E. P. Coomes

Battelle Pacific Northwest Lab.
P.O. Box 999
Richland, WA 99352
Attn: B. M. Johnson

Battelle Pacific Northwest Lab.
P. O. Box 999
Richland, WA 99352
Attn: W. J. Krotiuk

Battelle Pacific Northwest Lab.
P. O. Box 999
Richland, WA 99352
Attn: W. J. Widrig

Boeing Company
P.O. Box 3999
MS 8K-30
Seattle, WA 98124-2499
Attn: Dr. A. Sutey

Boeing Company
Boeing Aerospace System
P.O. Box 3707
Seattle, WA 98124
Attn: K. Kennerud

Brookhaven National Laboratory
P.O. Box 155
Upton, NY 11973
Attn: T. Bowden

Brookhaven National Laboratory
P.O. Box 155
Upton, NY 11973
Attn: H. Ludewig

Brookhaven National Laboratory
P.O. Box 155
Upton, NY 11973
Attn: Dr. W. Y. Kato

Brookhaven National Laboratory
Bldg. 701, Level 143
MS 820M
P.O. Box 155
Upton, NY 11973
Attn: Dr. J. Powell

California Inst. of Technology
Jet Propulsion Laboratory
4800 Oak Grove Drive
Pasadena, CA 91109
Attn: V. C. Truscello

Jet Propulsion Laboratory
4800 Oak Grove Drive
MS 122-123
Pasadena, CA 91109
Attn: P. Bankston

California Inst. of Technology
Jet Propulsion Laboratory
MS 502-307
4800 Oak Grove Drive
Pasadena, CA 91109
Attn: E. P. Framan

California Inst. of Technology
Jet Propulsion Laboratory
MS 264-770
4800 Oak Grove Drive
Pasadena, CA 91109
Attn: L. Isenberg

California Inst. of Technology
Jet Propulsion Laboratory
4800 Oak Grove Drive
Pasadena, CA 91109
Attn: J. Mondt

DARPA
1400 Wilson Blvd.
Arlington, VA 22209
Attn: P. Kemmey

DCSCON Consulting
4265 Drake Court
Livermore, CA 94550
Attn: D. C. Sewell

Defense Nuclear Agency
6801 Telegraph Road
Alexandria, VA 22310-3398
Attn: J. Farber/RAEV

DNA/RAEV
6801 Telegraph Road
Alexandria, VA 22310-3398
Attn: J. Foster

EG&G Idaho, Inc./INEL
P.O. Box 1625
Idaho Falls, ID 83415
Attn: R. Rice

EG&G Idaho, Inc./INEL
P.O. Box 1625
Idaho Falls, ID 83415
Attn: J. Dearien

EG&G Idaho, Inc./INEL
P.O. Box 1625
Idaho Falls, ID 83415
Attn: M. L. Stanley

EG&G Idaho, Inc./INEL
P.O. Box 1625
Idaho Falls, ID 83415
Attn: R. D. Struthers

EG&G Idaho, Inc./INEL
P.O. Box 1625
Idaho Falls, ID 83415
Attn: J. F. Whitbeck

EG&G Idaho, Inc./INEL
P.O. Box 1625
Idaho Falls, ID 83415
Attn: P. W. Dickson

EG&G Idaho, Inc./INEL
P.O. Box 1625
Idaho Falls, ID 83415
Attn: J. W. Henscheid

Ford Aerospace Corporation
Aeronutronic Div.
Ford Road, P.O. Box A
Newport Beach, CA 92658-9983
Attn: V. Pizzuro

GA Technologies
P.O. Box 85608
San Diego, CA 92138
Attn: H. J. Snyder

GA Technologies
P.O. Box 85608
San Diego, CA 92138
Attn: C. Fisher

GA Technologies
P.O. Box 85608
San Diego, CA 92138
Attn: Dr. R. Dahlberg

Garrett Fluid Systems Co.
P.O. Box 5217
Phoenix, AZ 85010
Attn: Robert Boyle

General Electric
P. O. Box 8555
Astro Systems
Philadelphia, PA 19101
Attn: Dr. R. J. Katucki

General Electric NSTO
310 DeGuigne Drive
Sunnyvale, CA 90486
Attn: E. E. Gerrels

General Electric NSTO
310 DeGuigne Drive
Sunnyvale, CA 90486
Attn: H. S. Bailey

General Electric-SCO
P. O. Box 8555
35T15, Bldg. 20
Astro Systems
Philadelphia, PA 19101
Attn: J. Chan

General Electric
P. O. Box 8555
Bldg. 100, Rm M2412
Astro Systems
Philadelphia, PA 19101
Attn: J. Hnat

General Electric
P. O. Box 8555
Astro Systems
Philadelphia, PA 19101
Attn: R. D. Casagrande

General Electric
P. O. Box 8555
Astro Systems
Philadelphia, PA 19101
Attn: W. Chiu

Grumman Aerospace Corporation
MS B20-05
Bethpage, NY 11714
Attn: J. Belisle

House of Representatives Staff
Space and Technology Committee
2320 Rayburn Building
Washington, DC 20515
Attn: Tom Weimer

202 NSC
University of Florida
Gainesville, FL 32611
Attn: N. J. Diaz

International Energy Assoc. Ltd.
1717 Louisiana NE
Suite 202
Albuquerque, NM 87110
Attn: W. H. Roach

International Energy Assoc. Ltd.
1717 Louisiana NE
Suite 202
Albuquerque, NM 87110
Attn: G. B. Varnado

Lawrence Livermore National Lab.
P. O. Box 808
Livermore, CA 94550
Attn: Lynn Cleland, MS L-144

Lawrence Livermore National Lab.
P. O. Box 808
Livermore, CA 94550
Attn: C. E. Walter, MS L-144

Los Alamos National Laboratory
P. O. Box 1663
Los Alamos, NM 87545
Attn: T. Trapp, MS-E561

Los Alamos National Laboratory
P. O. Box 1663
Los Alamos, NM 87545
Attn: R. Hardie, MS-F611

Los Alamos National Laboratory
P. O. Box 1663
Los Alamos, NM 87545
Attn: C. Bell, MS F611

Los Alamos National Laboratory
P. O. Box 1663
Los Alamos, NM 87545
Attn: R. J. LeClaire, MS F611

Los Alamos National Laboratory
P. O. Box 1663
Los Alamos, NM 87545
Attn: S. Jackson, MS-F611

Los Alamos National Laboratory
P. O. Box 1663
Los Alamos, NM 87545
Attn: J. Metzger

Los Alamos National Laboratory
P. O. Box 1663
Los Alamos, NM 87545
Attn: C. W. Watson, MS-F607

Los Alamos National Laboratory
P. O. Box 1663
Los Alamos, NM 87545
Attn: Don Reid, MS-H811

Los Alamos National Laboratory
P. O. Box 1663
Los Alamos, NM 87545
Attn: R. Bohl, MS-K560

Los Alamos National Laboratory
P. O. Box 1663
Los Alamos, NM 87545
Attn: D. R. Bennett

Los Alamos National Laboratory
P. O. Box 1663
Los Alamos, NM 87545
Attn: W. L. Kirk

Los Alamos National Laboratory
P. O. Box 1663
Los Alamos, NM 87545
Attn: M. Merrigan

Los Alamos National Laboratory
P. O. Box 1663
Los Alamos, NM 87545
Attn: T. P. Suchocki

Los Alamos National Laboratory
P. O. Box 1663
Los Alamos, NM 87545
Attn: L. H. Sullivan

Martin Marietta Corp.
P. O. Box 179
Denver, CO 80201
Attn: R. Giellis, MS 0484

Martin Marietta Corp.
P. O. Box 179
Denver, CO 80201
Attn: R. Zercher
MSL8060

Massachusetts Institute of
Technology
1328 Albany Street
Cambridge, MA 02139
Attn: Dr. J. A. Bernard

NASA Lewis Research Center
21000 Brookpark Road
Cleveland, OH 44135
Attn: J. Winter, MS 301-5

NASA Lewis Research Center
21000 Brookpark Road
Cleveland, OH 44135
Attn: Barbara McKissock, MS 301-5

NASA Lewis Research Center
21000 Brookpark Road
Cleveland, OH 44135
Attn: A. Juhasz
MS 301-5, Rm. 101

NASA Lewis Research Center
21000 Brookpark Road
Cleveland, OH 44135
Attn: J. Smith, MS 301-5

NASA Lewis Research Center
21000 Brookpark Road
Cleveland, OH 44135
Attn: H. Bloomfield
MS 301-5, Rm. 103

NASA Lewis Research Center
21000 Brookpark Road
Cleveland, OH 44135
Attn: Jim Bolander, 3350
Research/Technology Branch

NASA Lewis Research Center
21000 Brookpark Road
Cleveland, OH 44135
Attn: Kathleen Batke; 3350
Research/Technology Branch

NASA Lewis Research Center
21000 Brookpark Road
Cleveland, OH 44135
Attn: C. Purvis
MS 302-1, Rm. 101

NASA Lewis Research Center
21000 Brookpark Road
Cleveland, OH 44135
Attn: D. Bents, MS 301-5

NASA Lewis Research Center
21000 Brookpark Road
Cleveland, OH 44135
Attn: I. Myers
MS 301-2, Rm 116

NASA Lewis Research Center
21000 Brookpark Road
Cleveland, OH 44135
Attn: G. Schwarze MS 301-2, Rm. 117

NASA Lewis Research Center
21000 Brookpark Road
Cleveland, OH 44135
Attn: J. Sovie MS 301-5, Rm. 105

National Research Council
Energy Engineering Board
Commission on Engineering
and Technical Systems
2101 Constitution Avenue
Washington, DC 20418
Attn: R. Cohen

Naval Research Laboratory
Washington, DC 20375-5000
Attn: R. L. Eilbert

Naval Research Laboratory
Washington, DC 20375-5000
Attn: I. M. Vitkovitsky

Naval Space Command
Dahlgren, VA 22448
Attn: Commander R. Nosco

Naval Space Command
N5
Dahlgren, VA 22448
Attn: Maj. J. Wiley

Naval Space Command
Dahlgren, VA 22448
Attn: Mr. B. Meyers

Naval Surface Weapons Center
Dahlgren, VA 22448-5000
Attn: R. Gripshoven-F12

Naval Surface Weapons Center
Dahlgren, VA 22448-5000
Attn: R. Dewitt-F12

White Oak Laboratory
Silver Springs, MD 20903-500
MC R-42
Attn: B. Maccabee

Nichols Research Corp.
2340 Alamo Street, SE
Suite 105
Albuquerque, NM 87106
Attn: R. Weed

Oak Ridge National Laboratory
P. O. Box Y
Bldg. 9201-3, MS-7
Oak Ridge, TN 37831
Attn: J. P. Nichols

Oak Ridge National Laboratory
P. O. Box Y
Bldg. 9201-3, MS-7
Oak Ridge, TN 37831
Attn: D. Bartine

Oak Ridge National Laboratory
P. O. Box X
Oak Ridge, TN 37831
Attn: H. W. Hoffman

Oak Ridge National Laboratory
P. O. Box Y
Bldg. 9201-3, MS-7
Oak Ridge, TN 37831
Attn: R. H. Cooper, Jr.

Oak Ridge National Laboratory
P. O. Box Y
Bldg. 9201-3, MS-7
Oak Ridge, TN 37831
Attn: J. C. Moyers

Oak Ridge National Laboratory
P. O. Box Y
Oak Ridge, TN 37831
Attn: M. Olszewski

Oak Ridge National Laboratory
P. O. Box Y
Bldg. 9201-3, MS-7
Oak Ridge, TN 37831
Attn: M. Siman-Tov

Oak Ridge National Laboratory
P. O. Box Y
Bldg. 9201-3, MS-7
Oak Ridge, TN 37831
Attn: F. W. Wiffen

RADC/OCTP
Griffiss AFB
New York 13441
Attn: R. Gray

Riverside Research Institute
1701 No. Ft. Meyers Drive
Suite 700
Arlington, VA 22209
Attn: J. Feig

Science & Engineering Associates
6301 Indian School Road, NE
Albuquerque, NM 87110
Attn: G. L. Zigler

SDI Organization
The Pentagon
Washington, DC 20301-7100
Attn: R. Verga

SDI Organization
The Pentagon
Washington, DC 20301-7100
Attn: D. Buden

SDI/SLKT
The Pentagon
1717 H. St. NW
Washington, D. C. 20301
Attn: C. Northrup

SDIO/DE
Washington, DC 20301-7100
Attn: Dr. R. Hammond

SDIO/IST
Washington, DC 20301-7100
Attn: Dr. L. Cavery

SDIO/KE
The Pentagon
Washington, DC 20301-7100
Attn: Col. R. Ross

SDIO
The Pentagon
Washington, DC 20301-7100
Attn: Maj. R. X. Lenard

SDIO/SATKA
Washington, DC 20301-7100
Attn: Col. Garry Schnelzer

SDIO/SY
Washington, DC 20301-7100
Attn: Dr. C. Sharn

SDIO/SY
Washington, DC 20301-7100
Attn: Col. J. Schofield

SDIO/SY
Washington, DC 20301-7100
Attn: Col. J. Graham

SDIO/SY
Washington, DC 20301-7100
Attn: Capt. J. Doegan

Space Power, Inc.
1977 Councourse Dr.
San Jose, CA 95131
Attn: J. R. Wetch

State University of New York
at Buffalo
Dept. of Elec. Engineering
312 Bonner Avenue
Buffalo, NY 14260
Attn: Jim Sargeant

TRW
One Space Park
Redondo Beach, CA 90278
Attn: R. L. Hammel

TRW
One Space Park
Redondo Beach, CA 90278
Attn: T. Fitzgerald

TRW
One Space Park
Redondo Beach, CA 90278
Attn: James Garner

One Space Park
Redondo Beach, CA 90278
Attn: B. Glasgow

TRW
One Space Park
Redondo Beach, CA 90278
Attn: A. D. Schoenfeld

Teledyne Brown Engineering
Cummings Research Park
Huntsville, AL 35807
Attn: Dan DeLong

Texas A&M University
Nuclear Engineering Dept.
College Station, TX 77843-3133
Attn: F. Best

Texas Tech. University
Dept. of Electrical Engr.
Lubbock, TX 79409
Attn: Dr. W. Portnoy

U. S. Army ARDC
Building 329
Picatinny Arsenal
New Jersey 87806-5000
Attn: SMCAR-SSA-E

U. S. Army Belvoir RDE Center
Fort Belvoir, VA 22060-5606
Attn: Dr. L. Amstutz-STRABE-FGE

U. S. Army Lab. Com.
SLKET/ML
Pulse Power Technology Branch
Fort Monmouth, NJ 07703-5000
Attn: S. Levy

U. S. Army Lab. Com.
SLKET/ML
Pulse Power Technology Branch
Fort Monmouth, NJ 07703-5000
Attn: N. Wilson

U. S. Army Strategic Defense Com.
106 Wynn Drive
Huntsville, AL 35807
Attn: C. Cooper

U. S. Army Strategic Defense Com.
106 Wynn Drive
Huntsville, AL 35807
Attn: G. Edlin

U. S. Army Strategic Defense Com.
106 Wynn Drive
Huntsville, AL 35807
Attn: R. Hall

U. S. Army Strategic Defense Com.
106 Wynn Drive
Huntsville, AL 35807
Attn: E. L. Wilkinson

U. S. Army Strategic Defense Com.
106 Wynn Drive
Huntsville, AL 35807
Attn: D. Bouska

U. S. Army Strategic Defense Com.
106 Wynn Drive
Huntsville, AL 35807
Attn: W. Sullivan

U. S. Army Strategic Defense Com.
106 Wynn Drive
Huntsville, AL 35807
Attn: F. King

U. S. Department of Energy
Chicago Operations Office
9800 S. Cass Avenue
Argonne, IL 60439
Attn: J. L. Hooper

U. S. Department of Energy
NE-52
GTN
Germantown, MD 20545
Attn: J. Warren

U. S. Department of Energy
NE-54
F415/GTN
Germantown, MD 20545
Attn: E. Wahlquist

U. S. Department of Energy
NE-521
Germantown, MD 20874
Attn: D. Bennett

San Francisco Operations Office
1333 Broadway Ave,
Oakland, CA 94612
Attn: J. K. Hartman

U. S. Department of Energy
SAN - ACR Division
1333 Broadway
Oakland, CA 94612
Attn: J. Krupa

U. S. Department of Energy
SAN - ACR Division
1333 Broadway
Oakland, CA 94612
Attn: W. Lambert

U. S. Department of Energy
SAN - ACR Division
1333 Broadway
Oakland, CA 94612
Attn: J. Zielinski

U. S. Department of Energy
Pittsburgh Energy Tech. Center
P.O. Box 18288
Pittsburgh, PA 15236
Attn: G. Staats (PM-20)

U. S. Department of Energy
NE-54
Washington, DC 20545
Attn: I. Helms

U. S. Department of Energy
Oak Ridge Operations Office
P.O. Box E
Oak Ridge, TN 37830
Attn: E. E. Hoffman

U. S. Department of Energy
Washington, DC 20545
Attn: S. J. Lanes

U. S. Department of Energy
MA 206
Washington, DC 20545
Attn: J. P. Lee

U. S. Department of Energy
San Francisco Operations Office
1333 Broadway Avenue
Oakland, CA 94612
Attn: S. L. Samuelson

U. S. Department of Energy
ALO/ETD
P.O. Box 5400
Albuquerque, New Mexico 87115
Attn: R. L. Holton

U. S. Department of Energy
ALO/ETD
P.O. Box 5400
Albuquerque, New Mexico 87115
Attn: C. Quinn

U. S. Department of Energy/Idaho
785 DOE Place
Idaho Falls, ID 83402
Attn: P. J. Dirkmaat

United Technologies
International Fuel Cells
195 Governor's Highway
South Windsor, CT 06074
Attn: D. McVay

United Technologies
International Fuel Cells
195 Governor's Highway
South Windsor, CT 06074
Attn: J. L. Preston, Jr.

United Technologies
International Fuel Cells
195 Governor's Highway
South Windsor, CT 06074
Attn: J. C. Trocciola

University of Missouri - Rolla
220 Engineering Research Lab
Rolla, MO 65401-0249
Attn: A. S. Kumar

University of New Mexico
Chemical and Nuclear Engineering
Department
Albuquerque, NM 87131
Attn: M. El-Genk

University of Wisconsin
Fusion Technology Institute
1500 Johnson Drive
Madison, WI 53706-1687
Attn: Gerald Kulcinski

W. J. Schafer Associates
1901 No. Ft. Myers Drive
Suite 800
Arlington, VA 22209
Attn: P. Mace

W. J. Schafer Associates
1901 No. Ft. Myers Drive
Suite 800
Arlington, VA 22209
Attn: Ormon Bassett

W. J. Schafer Associates
1901 No. Ft. Myers Drive
Suite 800
Arlington, VA 22209
Attn: M. Nikolich

W. J. Schafer Associates
1901 No. Ft. Myers Drive
Suite 800
Arlington, VA 22209
Attn: J. Crissey

W. J. Schafer Associates
2000 Randolph Road, SE
#205
Albuquerque, NM 87106
Attn: D. C. Straw

W. J. Schafer Associates
1901 No. Ft. Myers Drive
Suite 800
Arlington, VA 22209
Attn: A. K. Hyder

Westinghouse Electric
P. O. Box 158
Madison, PA 15663-0158
Attn: J. Chi

Westinghouse
Advanced Energy Systems Division
Manager, Space & Defense Program
Route 70, Madison Exit
Madison, PA 15663
Attn: J. F. Wett

Westinghouse
Advanced Energy Systems Division
P.O. Box 158
Madison, PA 15663
Attn: Dr. J. W. H. Chi

1310 Beulah Road
Bldg. 501-3Y56
Pittsburgh, PA 15235
Attn: J. R. Repp

Westinghouse R&D
1310 Beulah Road
Bldg. 501-3Y56
Pittsburgh, PA 15235
Attn: L. Long

Westinghouse R&D
1310 Beulah Road
Bldg. 501-3Y56
Pittsburgh, PA 15235
Attn: Owen Taylor

Westinghouse Advanced Energy
Systems Division
P.O. Box 158
Madison, PA 15663
Attn: G. Farbman

Westinghouse Hanford Company
P. O. Box 1970
Richland, WA 99352
Attn: D. S. Dutt

Westinghouse Hanford Company
P. O. Box 1970
Richland, WA 99352
Attn: B. J. Makenas

1140 P. S. Peercy
1200 J. P. Van Devender
1240 K. R. Prestwich
1248 M. T. Buttram
1270 R. B. Miller
1271 M. J. Clauser
1512 D. J. Rader
1800 R. L. Schwoebel
1810 G. G. Kepler
1830 M. J. Davis
1832 W. B. Jones
1832 R. J. Salzbrenner
1840 R. J. Eagan
2110 R. E. Bair
2120 E. G. Franzek
2140 C. F. Gibbon
2150 E. D. Graham, Jr.
2560 J. T. Cutchen
3141 S. A. Landenberger (5)
3151 W. L. Garner (3)
3154-1 C. H. Dalin
(28 for DOW/OSTI)
6400 D. J. McCloskey
6410 N. R. Ortiz
6420 J. V. Walker
6421 P. S. Pickard
6422 J. E. Brockman
6425 W. J. Camp
6431 J. S. Philbin
6440 D. A. Dahlgren
6450 T. R. Schmidt
6500 A. W. Snyder
6510 W. B. Gauster
6511 L. O. Cropp
6511 M. W. Edenburn
6511 D. R. Gallup
6511 S. L. Hudson
6511 A. C. Marshall
6511 W. H. McCulloch
6511 P. J. McDaniel
6511 R. E. Pepping
6511 F. V. Thome
6512 D. M. Ericson, Jr. (5)
6512 F. J. Wyant
6512 M. S. Chu
6512 D. Dobranich (10)
6512 V. J. Dandini
8024 P. W. Dean
8400 R. C. Wayne
9000 R. L. Hagengruber

9010 W. C. Hines
9012 J. W. Keizur
9012 L. W. Connell
9012 R. M. Zazworski
9100 R. G. Clem
9110 P. A. Stokes
9140 D. J. Rigali